ELSEVIER

Journal of Molecular Structure (Theochem) 572 (2001) 203–212

THEO CHEM

www.elsevier.com/locate/theochem

A CIS study of solvent effects on the electronic absorption spectrum of Reichardt's dye

P.G. Jasien*, L.L. Weber

Department of Chemistry, California State University—San Marcos, San Marcos, CA 92096-0001, USA

Received 9 April 2001; revised 18 June 2001; accepted 19 June 2001

Abstract

A configuration interaction singles wavefunction, in conjunction with a self-consistent reaction field and a simple Onsager spherical cavity model, has been used to calculate the solvent induced shifts in Reichardt's dye (RD). The results from this simple method are in good agreement with experiment for aprotic solvents, but large discrepancies exist for protic solvents. This discrepancy can be partially compensated for by including one explicit solvent molecule H-bonded to RD. Geometry optimization of the S_1 state in RD predicts a pyramidal sp^3 hybridized N atom and an overall structure that differs significantly from that in the S_0 state. Analysis of the calculated dipole moments and selected molecular orbitals are in accord with previous analyses of the $S_0 \rightarrow S_1$ charge transfer transition in RD. However, the nature of the $S_0 \rightarrow S_2$ transition appears to change with solvent dielectric strength (ϵ). At low ϵ this transition seems to have significant charge transfer character that decreases as ϵ increases.

Keywords: Excited state; Solvent effects; Configuration interaction singles; Electronic spectra; Reichardt's dye

1. Introduction

Reichardt's Dye (RD), also known as Betaine-30 or 2,6-diphenyl-4-(2,4,6-triphenyl-N-pyridinio)phenolate, is a betaine dye with a large solvatochromatic shift in the lowest energy electronic transition. This transition has been attributed to an intramolecular $\pi \rightarrow \pi^*$ charge transfer (CT) excitation in the molecule and has one of the largest known solvent induced shifts [1]. Due to the large solvent dependent shift of this transition, the properties of RD have been carefully studied in terms of their correlation with solvent [1–5] and theoretically [6–12].

The large negative solvatochromatism in RD is due to the highly dipolar nature of the ground state and the much less polar nature of the first excited state. The origin of the dipolar ground state can be seen from the simple structure of the molecule shown in Fig. 1 that shows a formal negatively charged phenolate system and a positively charged pyridinium ring. The ground state electric dipole moment (μ) of RD has been measured in 1,4-dioxane as 14.8 ± 1.2 D and is consistent with a dipolar structure [13,14]. The excited state μ has also been measured as 6.2 ± 0.3 D in the same solvent [13] and clearly demonstrates the large intramolecular CT in this molecule upon excitation. The electronic spectrum of RD is particularly sensitive to electron pair acceptor solvents due to the accessible lone pair on the oxygen of the phenolate. On the other hand, the formally positive N on the pyridinium

* Corresponding author. Tel.: +1-760-750-4135; fax: +1-760-750-4111.

E-mail address: jasien@csusm.edu (P.G. Jasien).

0166-1280/01/$ - see front matter
PII: S0166-1280(01)00634-0

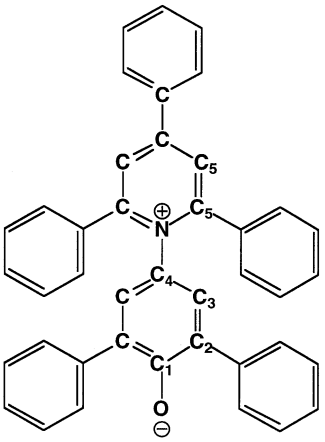

Fig. 1. Schematic representation of bonding in RD.

ring does not interact strongly with solvent molecules since it is quite shielded by the bulky groups surrounding it [12].

The large sensitivity of the lowest energy electronic transition in RD has made it a good candidate for probing the polarity of the solvent medium. In fact, the ET-30 scale [1,3,5] has been developed and used to indicate bulk solvent polarity, as well as the local or nonlocal nature of the solvation [15]. This scale has also been used as an indicator of the solvent environment of micelles, microemulsions, and phospholipid bilayers [16].

Previous theoretical work on RD has included an investigation by Jano [6] in which measured electronic transition energies and a multiple regression procedure were used to test an empirical model for solvent shifts. Detailed theoretical analyses of the solvation in RD by Matyushov et al. [7] and Perng et al. [8] have also been performed. The investigation by Matyushov et al. [7] used a first principles approach and sought to partition the specific solute–solvent interactions in terms of induction, dispersion, and dipole–dipole forces. A major conclusion of this study was that dispersion effects on the solvent shift are important contributors even in very polar solvents.

A number of recent studies have combined quantum mechanical calculations with a variety of solvent models to investigate this system. Bartkowiak and Lipinski used their Langevin dipoles/Monte Carlo model and a sum-over-states formalism to calculate the conformational and solvent dependence of the first molecular hyperpolarizability of RD [9]. Lobaugh and Rossky used a semiempirical Pariser–Parr–Pople Hamiltonian and a quantum molecular dynamics methodology to study the excited state dynamics of RD in acetonitrile [10]. In a separate study these authors used a similar method to study the effect of torsional modes on the electronic absorption spectrum in the same solvent [11]. Work by Mente and Maroncelli used a combination of Monte Carlo methods and ab initio and semiempirical quantum mechanical methods to explore the geometry and charge distribution of RD and its effect on the absorption spectrum [12]. Very recently, Ishida and Rossky have used the RISM-SCF method to study the ground state structure and properties of a smaller related betaine dye molecule in acetonitrile and water [17].

In this work, we investigated the nature of the lowest two excited states of RD and the solvent dependence of the electronic spectrum. Ab initio calculations at the restricted Hartree–Fock (RHF) level, in conjunction with the Self-Consistent Reaction Field (SCRF) formalism and the configuration interaction singles (CIS) methods [18,19] were used to extract the relevant information. As in a previous report [20], we used a simple Onsager spherical cavity model (OM) [21,22] to represent the non-specific effects of the solvent. In that previous study, this simple method that treats the solvent as a continuum proved to be sufficient to describe the relative solvent shifts in non-H-bonding solvents. It was found that implementing the more 'accurate' treatment of the solute shape via the isodensity polarized continuum model (IPCM) did not lead to better agreement of the predicted values with those from experiment. In the present work, we have also investigated a modification of the simple OM by explicitly including one or more solvent molecules into the system before embedding the solute in the solvent medium.

2. Computational

Calculations were performed using the Gaussian 94 [23] program. Molecular orbital (MO) plots were generated using the MacSpartan Plus program [24]. Due to the size of the molecule studied and the computational facilities available, the basis set chosen was a compromise between accuracy and

Table 1
Comparison of the basis set dependence of ΔE(eV), oscillator strengths (f), and electric dipole moments (μ in D) (the symbols 0, 1, and 2 denote the ground, first excited, and second excited states)

Basis set	ΔE_{01}	ΔE_{02}	f_1	f_2	μ_0	μ_1
3-21G	2.90	4.15	0.15	0.14	17.90	1.64
6-31G	3.02	4.20	0.15	0.17	18.23	1.92
6-31G*	3.03	4.14	0.15	0.19	17.74	1.70

computational expense. The unpolarized 3-21G basis set [25] was used for most calculations in this work, although selected calculations were performed with the 6-31G and the polarized 6-31G* basis sets [26].

All calculations were carried out using an RHF wavefunction as a reference. Geometry optimizations were performed at the RHF/3-21G level. Structures were converged to 0.001 Å for bond lengths and 0.1° for bond angles in each simulated solvent environment. Some dihedral angles may not be converged to this extent, owing to the flatness of the potential energy surface for the coordinate. Geometry optimizations in the presence of solvent were performed using an SCRF wavefunction with the OM [21,22] as implemented in the Gaussian 94 program [18,23]. The solvent dielectric constants (ϵ) chosen (2, 5, 9, 20, 24, 33, 38, 47, and 79) roughly correspond to those for the solvents: n-hexane, chloroform, methylene chloride, acetone, ethanol, methanol, acetonitrile, dimethyl sulfoxide, and water, respectively [27]. The majority of these solvents are aprotic and cannot H-bond to the solute. In these cases, the use of a continuum model for the solvent may be quite appropriate. The H-bonding solvents with $\epsilon = 24$, 33, and 79 were included to study local effects on solvation. In addition to the general OM implemented in this work, a series of calculations with the H-bonding solvents was done in which an individual solvent molecule was hydrogen bonded to the phenolate oxygen atom. The relative bulkiness of RD hinders direct solvation to the N atom in this molecule, however, the O site is readily open for hydrogen-bonding. In fact, an X-ray crystal structure of the 4-bromo substituted derivative of RD (recrystallized from ethanol) shows a coordinated ethanol molecule in very close proximity to the phenolate oxygen [28].

Table 2
Comparison of calculated solvent shifts for 6-31G and 3-21G basis sets (the symbols 0, 1, and 2 denote the ground, first excited, and second excited states)

ϵ	ΔE_{01}(321G)	ΔE_{01}(631G)	ΔE_{02}(321G)	ΔE_{02}(631G)
2	0.00	0.00	0.00	0.00
5	0.28	0.29	0.09	0.08
9	0.43	0.43	0.12	0.10
20	0.52	0.53	0.13	0.11

The procedure used for optimizing the geometry of RD in solvent involved an interative cycle of determining the solvent cavity radius (a_0) and geometry optimization as was described in Ref. [20]. Although the spherical cavity model is a large assumption in this work, the overall shape of RD is not that far from spherical, as can be seen from a space filling model (see for example fig. 2 in Ref. [12]).

Solvent effects in the excited state were implicitly included by using the ground state wavefunction and external electric field from the SCRF-RHF-OM calculation as the starting point for a CIS calculation [20]. This simple procedure neglects any solvent relaxation upon excitation. These calculations are designated CIS-SCRF-OM in this work. In all CIS calculations, the five lowest excited states were calculated, although only the lowest two will be discussed here.

3. Results and discussion

3.1. Basis set dependence

Given in Tables 1 and 2 are data that indicate the relative insensitivity of the calculated results on basis set. Test calculations indicated that the 3-21G basis set provided reasonable agreement with the excitation energies calculated using the larger 6-31G and 6-31G* basis sets for both the first and second excited states. This result is in agreement with the minor basis set dependence, going beyond a double zeta basis set, that was previously found for transitions involving valence-like excited states [29]. In the current calculations the predicted gas-phase lowest energy CIS excitation energy for the 3-21G, 6-31G, and 6-31G* basis sets of 2.90, 3.02, and 3.03 eV are all much larger than the extrapolated experimental value of 1.17 eV [6]. Such a deviation is expected since the

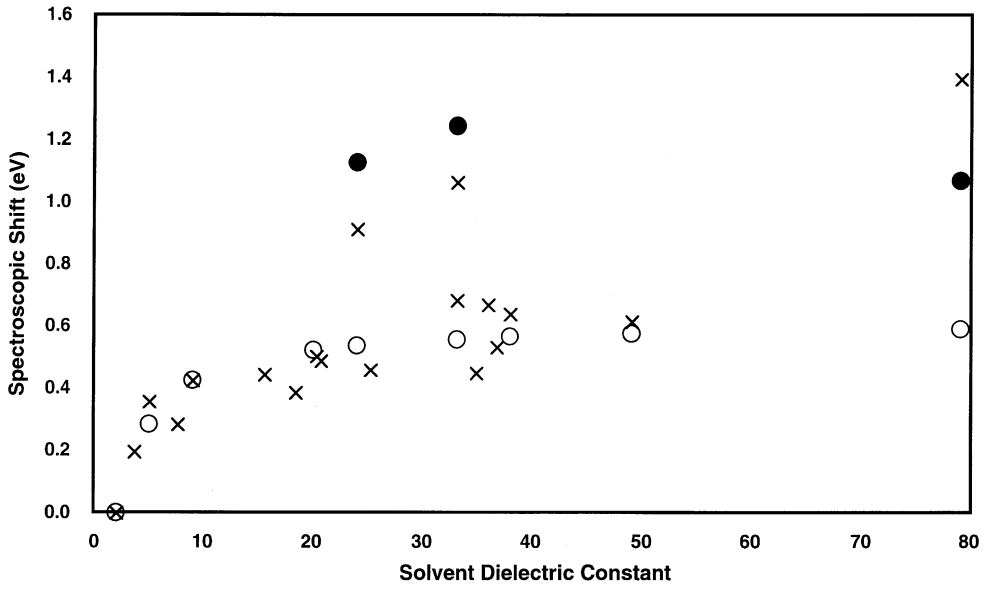

Fig. 2. Plot of calculated and experimental shifts for the $S_0 \rightarrow S_1$ electronic transition in RD (○, calculated; ×, experimental; ●, calculated with explicit solvent molecule). All values are referenced to $\epsilon = 2$.

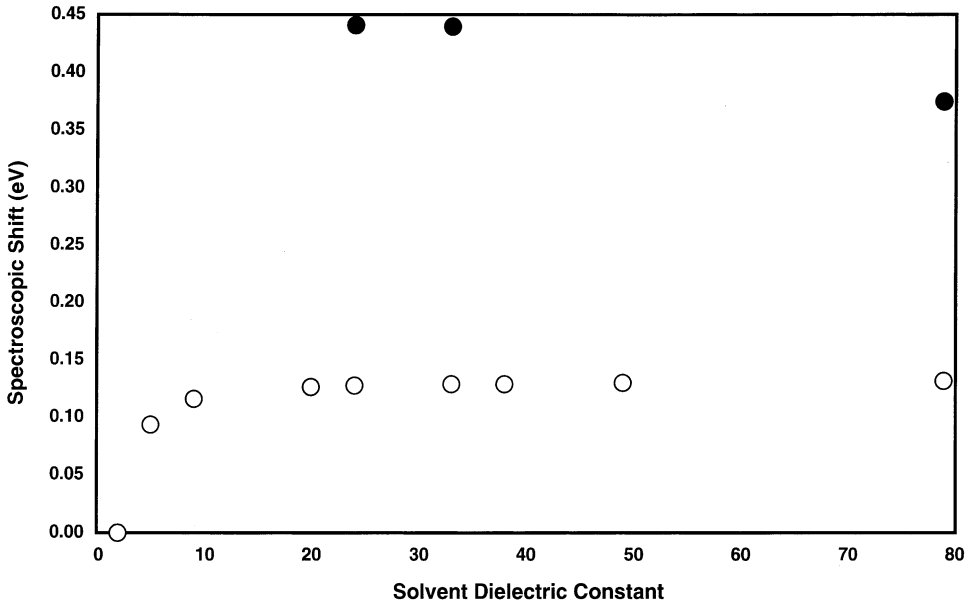

Fig. 3. Plot of calculated shifts for the $S_0 \rightarrow S_2$ electronic transition in RD (○, calculated; ●, calculated with explicit solvent molecule). All values are referenced to $\epsilon = 2$.

absolute values of the calculated excitation energies using the CIS method are known to overestimate the energy differences between ground and excited states [19]. The data in Table 2 show that although the absolute energy of the lowest two excitations differs somewhat with the 3-21G and 6-31G basis sets, the relative solvent shift is almost identical for these two basis sets.

The basis set effects on overall structure were not thoroughly investigated. However, a comparison of the calculated gas-phase structures for a related betaine dye molecule was done. The results in this betaine system from a larger DZP basis set [17] and those with the 3-21G basis set in this work yielded bond lengths for the pyridinium and phenolate ring systems that agreed to within 0.01 Å. The exception was the C—O length which differed by 0.015 Å. The torsional angle between the planes of the two rings was also in good agreement (38.4° for the 3-21G basis set and 39.9° for the DZP basis set).

3.2. Solvent effects on electronic absorptions

Fig. 2 shows a plot of the spectroscopic shift for the lowest energy excitation vs ϵ for the solvent for both calculated and experimental results. In both cases, the data are referenced to a solvent of $\epsilon = 2$. This was done to account for the known overestimation of the calculated excitation energies using the CIS method. Fig. 3 shows the solvent shift for the second excited state, also referenced to $\epsilon = 2$.

Although it has not been shown that the shifts would be the same if a larger basis set and more extensive electron correlation had been included into the wavefunction, the utility of the method used can be seen from the data. Fig. 2 shows very good agreement for the experimental and calculated solvent shifts for the lowest energy excitation in non-H-bonding solvents using the CIS-SCRF-OM model. The number of experimental points plotted shows that the calculated shifts fall well within the range of variation for these data. When comparing these data it is important to remember that the calculated excitation values have not included any effects due to the solvent response during the excitation. Therefore, these values can only be considered a rough estimate of the true transition energies.

For protic solvents the agreement with the simple OM is quite poor as expected for a solute molecule containing a site that can strongly interact with the solvent. The points plotted in Fig. 2 as filled circles for dielectric constants of 24, 33, and 79 represent the results of calculations using RD plus a single solvent molecule embedded in the OM spherical cavity. It can be seen that in all three cases, the addition of the lone coordinating solvent brought the calculated shifts into better agreement with those from the experiment, however, there are still significant discrepancies. In an effort to understand these differences, several other calculations were performed.

Since the SCRF-RHF-OM calculations with the 3-21G basis set would be expected to give shorter than expected H-bond lengths between the phenolate O and the solvent H atom, a simple check on the effect of the H-bond length was made. In the case of ethanol and methanol the solvent molecule was translated so that the O···O distance between RD and the solvent was equal to that determined from the experimental X-ray crystal structure of RD · ethanol. The experimental value for the O···O distance was 2.71 Å [28] while those found in the calculations for ethanol, methanol, and water were 2.65, 2.66, and 2.72 Å, respectively. In the case of ethanol, this modificaton led to a decrease in the predicted shift by 0.07 eV, bringing it in closer agreement with experiment. However, in the case of methanol, the effect was to increase the calculated shift by 0.03 eV and led to poorer agreement.

In the case of water, the discrepancy between the calculated and experimental shift is quite large. The current model predicts the solvent shift to be too small, in contrast to the results for methanol and ethanol. In the case of H_2O, supplemental calculations were done in which two additional water molecules were coordinated to the O atom of the coordinated water. The RD · $3H_2O$ system was then embedded in the spherical cavity and the geometry was optimized as described previously. The result from this calculation predicted a value for the shift that was too large. Therefore, although explicitly adding the extra water molecules increased the interaction, it leads to a result that overestimated the shift by as much as the calculation with one water underestimated it.

Fig. 3 shows that a similar pattern of spectroscopic shifts occurs for the $S_0 \rightarrow S_2$ excitation. In this case, the solvent shifts are much smaller than for the

Table 3
Calculated electric dipole moments, μ(D) for selected values of ϵ (the symbols 0, 1, and 2 denote the ground, first excited, and second excited states)

ϵ	μ_0	μ_1	μ_2
1	17.90	1.64	5.23
2	20.13	3.62	12.36
5	22.31	5.69	19.17
9	23.40	6.76	21.42
20	24.15	7.51	22.68
38	24.47	7.83	23.16
47	24.55	7.91	23.28

$S_0 \rightarrow S_1$ excitation. We could not find extensive experimental data reported for this excitation, so it is difficult gauge the accuracy of the calculated shifts. Although the relative shifts as a function of ϵ are smaller in this excitation, the calculational model that adds a lone solvent molecule to RD has a much larger percentage effect on the second excitation than the first.

The relatively good agreement of the experimental results with the CIS-SCRF-OM results from our work may seem to be inconsistent with the results of Matyushov et al. [7] in which it was concluded that solute-solvent dispersive effects play a significant role in determining the solvent induced shift in RD. However, close examination of their results show that although these dispersive effects are significant, they are essentially constant as a function of ϵ. Since our calculations are referenced to the $\epsilon = 2$ value, the major contribution of the dispersive effects that would be present are essentially subtracted out by the referencing. Therefore our model which includes only the dipolar interaction with the solvent is consistent with previous results.

3.3. Dipole moments and intensities

Given in Table 3 are selected values of μ calculated in this work. The calculated dipole moments are found to increase greatly with solvent, as was previously noted [11,12]. At the RHF level, calculated μ values are known to generally be too large for ground states. Here, the calculated value for the ground state, 20.1 D is about 36% larger than that measured in 1,4-dioxane, 14.8 ± 1.2 D. Surprisingly, Table 1 shows that the change in μ on going to a much larger 6-31G* basis set at the RHF level seems to be extremely small ($\Delta\mu = 0.16$ D). Therefore, the major error in the calculation of the dipole appears to arise, not from the basis set, but from the lack of extensive electron correlation. For the first excited state, the calculated electric dipole moment is found to be smaller than the

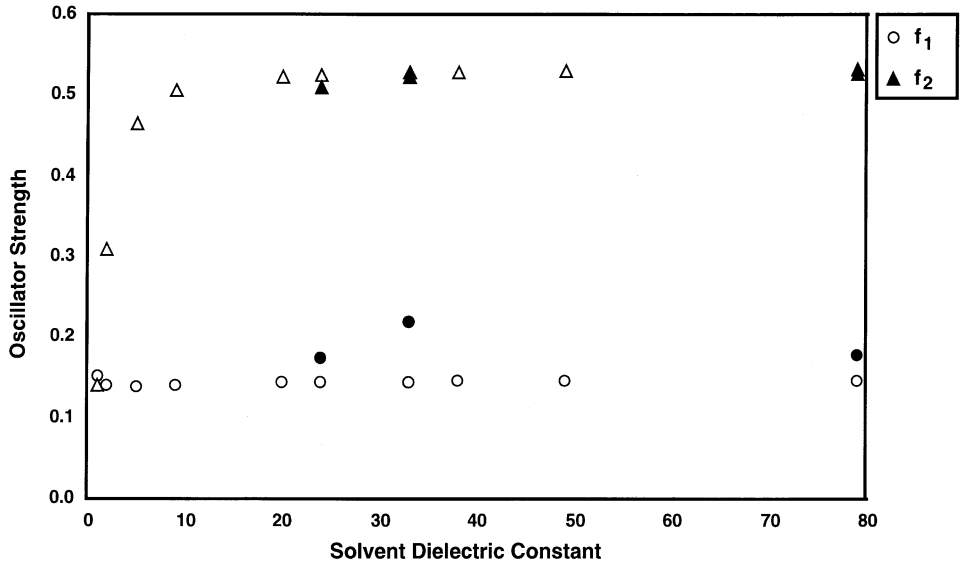

Fig. 4. Calculated values for oscillator strengths in RD (○, $S_0 \rightarrow S_1$; ●, $S_0 \rightarrow S_1$ with solvent molecule; △, $S_0 \rightarrow S_2$; ▲, $S_0 \rightarrow S_2$ with solvent molecule).

Table 4
Selected geometric parameters from RD calculations (all bond lengths in Å, angles in degrees)

State	ϵ	C_1-O	C_4-N	C_2-C_3	C_5-C_6	N-C_5	ϕ(C_5-N-C_4-C_3)	O···H-O
S_0	1	1.250	1.466	1.368	1.378	1.360	65.6	
	2	1.254	1.467	1.369	1.375	1.360	66.5	
	24	1.259	1.468	1.373	1.373	1.362	67.7	
	33	1.259	1.467	1.372	1.373	1.363	67.8	
	79	1.260	1.468	1.373	1.373	1.363	67.8	
	24 + EtOH	1.277	1.468	1.378	1.373	1.363		1.682
	33 + MeOH	1.278	1.468	1.377	1.370	1.364		1.688
	79 + H_2O	1.273	1.468	1.375	1.371	1.365		1.757
S_1	1	1.229	1.435	1.353	1.358	1.423		

experimental value, 3.62 D vs 6.2 ± 0.3 D, respectively. In this state as well, the calculated μ with a larger 6-31G* basis set leads to a small change as compared to the 3-21G basis set result at $\epsilon = 1$. The calculated values for μ in acetonitrile ($\epsilon = 38$) from the current work are in reasonable agreement with those of Lobaugh and Rossky [11]. They obtained values for μ of 24.95 D, 5.5 D, and 20.7 D for the S_0, S_1, and S_2 states, respectively, while those from the current work are 24.5, 7.8, and 23.2 D.

The dependence of μ on ϵ for the S_2 state is different than that for the S_0 or S_1 states. After starting out at a value close to that of the S_1state, the electric dipole moment for the S_2 state increases rapidly and is essentially the same as that for the ground state by $\epsilon = 20$. This may indicate some general change in the nature of the excited state as ϵ increases. (This possibility will be discussed later.)

Given in Fig. 4 are the calculated oscillator strengths (f_n) for the lowest energy transitions as a function of ϵ. The calculated oscillator strength for the $S_0 \rightarrow S_1$ excitation is predicted to show little dependence on ϵ. This result is not consistent with the results of Zong and McHale [30] and Kovalenko et al. [31] who measured a substantial increase in intensity on going from methanol to acetonitrile, instead of the decrease predicted in our calculations. As was mirrored in the large change in μ with ϵ for the S_2 state, the $S_0 \rightarrow S_2$ excitation is predicted to show a large initial increase in f as ϵ increases. The data indicate that although the $S_0 \rightarrow S_1$ and $S_0 \rightarrow S_2$ transitions would have comparable values of f at $\epsilon = 1$, by $\epsilon = 5$, the intensity of the $S_0 \rightarrow S_2$ excitation is predicted to be three times as large. Limited experimental data from our lab [32] seems to support the change in the ratio f_2/f_1 at low ϵ, but are not definitive.

3.4. Structure and structural changes

Table 4 lists selected structural parameters for RD at a number of different values of ϵ. These data show very small changes in the selected bond lengths as a function of ϵ. Suprisingly, the C_4-N distance is essentially constant over the full range of solvent dielectric strengths studied. The constant value of this distance is in contrast with the results of Ishida and Rossky for a similar betaine molecule [17]. In that case they predicted an increase of 0.018 Å in the phenolate–pyridinium C—N bond length upon going from the gas phase to acetonitrile. We do not believe that the constant value of the C_4—N distance in our calculations for RD is an artifact of the model. Use of our model on the betaine studied by Ishida and Rossky also predicts a substantial increase in this bond length. The difference in behavior of these two systems may be attributable to increased steric effects. In RD the C_4—N distance starts at a much longer 1.466 Å in the gas phase due to presence of the adjacent phenyl rings. Since this distance is so long to begin with, further lengthening cannot be induced by the solvent. This is consistent with the fact that no change occurs in this bond length even upon coordination of explicit solvent molecules.

As expected larger changes in the C_1—O bond length are seen in the cases where a lone solvent molecule is coordinated to the phenolate O. For methanol, ethanol, and water, these increases compared to the comparable ϵ continuum solvent models are 0.018, 0.019, and 0.013 Å, respectively.

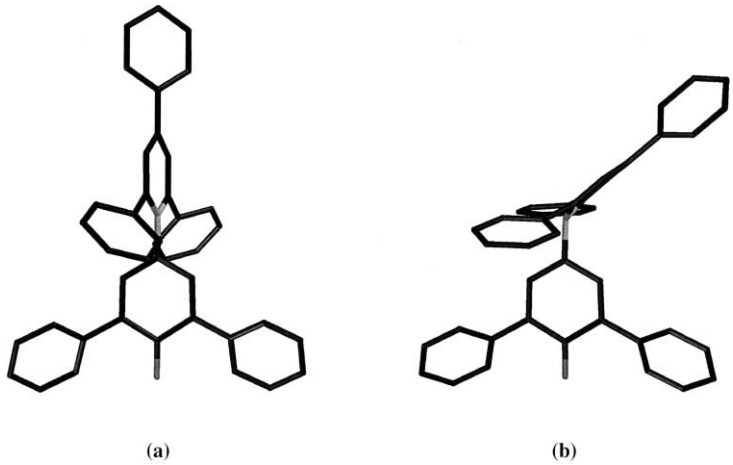

Fig. 5. Structures for the (a) S_0 and (b) S_1 states of RD, illustrating the overall structural change upon excitation.

The O···H hydrogen bond distance in the three calculations with the explicit solvent molecule are probably too short due to the small basis set used and the associated basis set superposition error [33]. The bond length of 1.682 Å for the O···H distance in the ethanol calculation corresponds to an O···O distance of 2.65 Å, which is shorter than the experimental distance from the X-ray structure of 2.71 Å [28].

In previous work [9,11], a great deal of effort has been expended in calculating properties of RD as a function of the torsion angle between the pyridinium and phenolate rings. In the current work, this angle changes very little as a function of solvent, from 65.6° at $\epsilon = 1$ to 67.8° at $\epsilon = 79$. Even the addition of the explicit solvent molecule increases this angle only by about 1°. The values of this torsional angle of between 66 and 68° are in good agreement with the value of 65° found in the experimental structure of Br substituted RD [28].

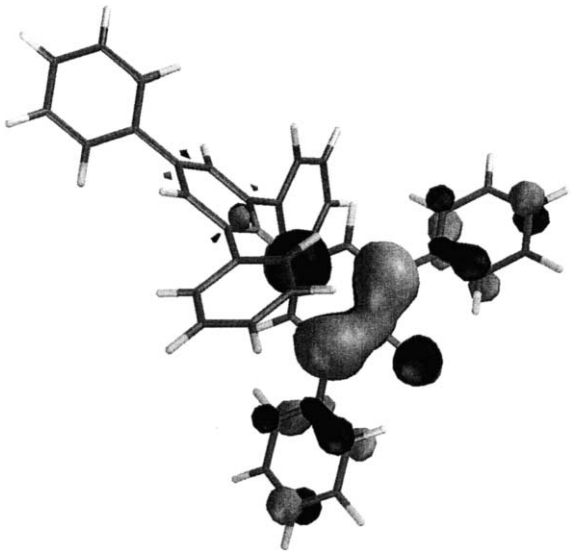

Fig. 6. Qualitative representation of the HOMO of RD from $\epsilon = 1$ calculation.

Substantial changes occur in the structure of RD when comparing the gas-phase structures for the S_0 and S_1 states. There are significant decreases in the C_1—O and C_4—N bond lengths of 0.021 and 0.031 Å. The C_2—C_3 and C_5—C_6 lengths also shorten by 0.015 and 0.020 Å. An extremely large increase of 0.063 Å occurs for the N—C_5 bond length. However, the most dramatic change in the structure is the pyramidalization of the N atom. These changes can be qualitatively seen from Fig. 5 and to our knowledge have not been noted previously. The phenolate and pyridinium rings in this structure lie almost perpendicular to each other. The resultant C—N bond lengths and the pyramidal N are consistent with an sp^3 hybridized N atom.

The changes in the bonding of RD upon going from the S_0 to the S_1 state are predicted to involve significant rearrangement of electron density (for example see fig. 1 in Ref. [30]). Predicted decreases in the C_1—O and C_4—N bond lengths are in accord with the development of more formal double bond

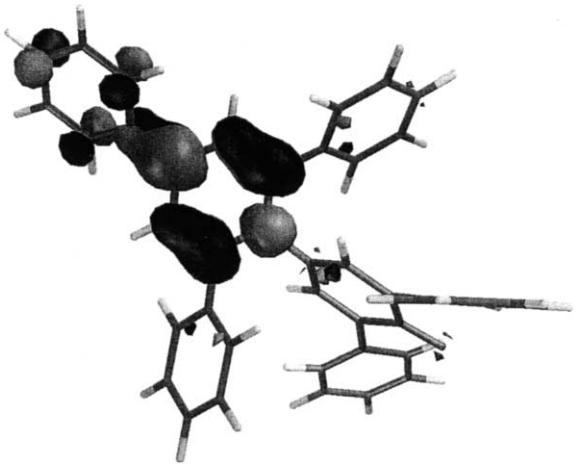

Fig. 7. Qualitative representation of the LUMO of RD from $\epsilon = 1$ calculation.

character, as are the shortening of the C_2—C_3 and C_5—C_6 bonds as they go from aromatic to formal double bonds. In addition, the increase of the N—C_5 bond is consistent with the structure as this bond goes from a formal aromatic C—N to a 'pure' single bond. However, the one major discrepancy with the current calculated structure and the formal bonding in the S_1 state is in the hybridization of the N atom. In terms of the overall bonding around N, an sp^2 hybridization would be expected, however, the pyramidal N atom predicted in our calculations is more consistent with an sp^3 hybridized N atom. While the exact geometric parameters for this excited state structure cannot be given at this level of calculation, we believe the CIS wavefunction with its limited correlation is capable of qualitatively describing the structural differences between the S_0 and the S_1 states.

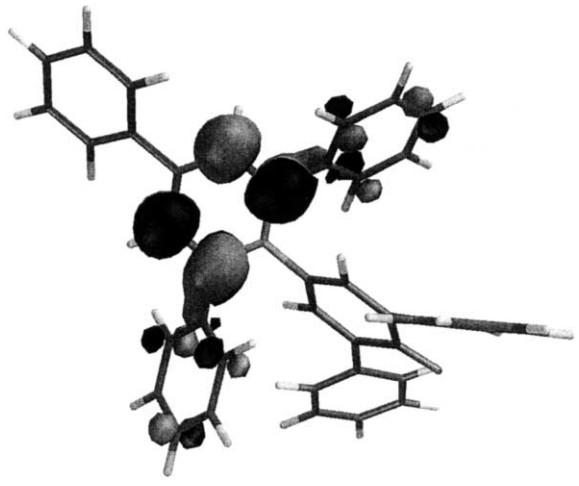

Fig. 8. Qualitative representation of the LUMO + 1 of RD from $\epsilon = 1$ calculation.

3.5. Nature of the electronic transitions

Analysis of the CIS results indicate that the wavefunction for the first excited state is dominated by a contribution from the HOMO → LUMO single excitation. For all values of ϵ studied, the coefficient for this single excitation is approximately 0.67. The HOMO from the $\epsilon = 1$ calculations is presented in Fig. 6 and clearly has a large contribution from atomic orbitals centered on the O and adjacent C atoms. On the other hand, the LUMO, presented in Fig. 7, shows negligible contribution from the atomic orbitals on these same centers. This is consistent with the large change in dipole moment from the S_0 to the S_1 state and the designation of this transition as CT in character.

Analysis of the S_2 wavefunction from the CIS calculations is somewhat more complex than that for the ground state. At $\epsilon = 1$ the S_2 wavefunction has a large contribution (coefficient of 0.65) for the HOMO → LUMO + 1 single excitation. However, this coefficient decreases to a smaller value (0.35) as ϵ increases. A full analysis of the wave function has not been done at other ϵ values, but it should be noted that the HOMO → LUMO + 1 contribution is also seen to a significant extent in the S_3 state which is calculated to have a negligible oscillator strength for the $S_0 \rightarrow S_3$ transition. The picture in Fig. 8 shows the LUMO + 1 at $\epsilon = 1$. It is seen that just as for the LUMO, the LUMO + 1 has negligible contribution from atomic centers on the phenolate ring and is dominated by contributions from centers on the pyridinium. However, whereas the LUMO had a contribution from the N center, this is absent in the LUMO + 1. In addition, the LUMO + 1 is predicted to be π anti-bonding with respect to all atomic centers on the pyridinium ring, in contrast to the LUMO orbital that was π bonding with respect to pyridinium ring carbons. The small dipole moment of this S_2 state at small ϵ and its rapid increase with ϵ indicates that the nature of the S_2 state changes from one with little CT character to one with increased dipolar character as ϵ increases. This is also consistent with the negligible

effect that the single coordinated solvent molecule has on the calculated f for the $S_0 \rightarrow S_2$ transition.

The question of the nature of the second excited state is discussed by Lobaugh and Rossky [11] in relation to the assignments made by Levinger et al. [34]. The experimental work seems to indicate that there are two closely spaced transitions assigned to $S_0 \rightarrow S_2$ and $S_0 \rightarrow S_3$. One of these transitions is CT in nature, while the other is a weak localized excitation. These results are consistent with the current calculations as discussed above, where there may be a change in the nature of the S_2 and S_3 states as a function of solvent ϵ. On the basis of the orbital analysis and the change in μ, the $S_0 \rightarrow S_2$ transition at low ϵ can also be classified as a CT type with a large $\pi \rightarrow \pi^*$ component, that decreases greatly in CT character as ϵ increases.

4. Conclusion

Calculations using a simple CIS-SCRF-OM method to calculate the solvent induced shifts in RD gives good agreement with experiment for aprotic solvents, but large discrepancies for protic ones. This discrepancy can be partially taken into account by explicitly including a single solvent molecule H-bonded to the phenolate O atom. Although improved in terms of the qualitative extent of the shift, the results are still not in good quantitative agreement. Inclusion of more water molecules explicitly in the calculations, showed a change consistent with the experimental results, however one water molecule underestimated and three water molecules overestimated the experimental shift. The optimized structure for the S_1 state in RD is predicted to have a pyramidal sp^3 hybridized N atom and an overall structure that differs significantly from that in the S_0 state. Analysis of the calculated dipole moments and selected molecular orbitals substantiate that there is a large CT in the $S_0 \rightarrow S_1$ transition in RD. However, the nature of the $S_0 \rightarrow S_2$ transition appears to change from one with a great deal of CT character at low ϵ to one with significantly decreased CT character at higher ϵ.

References

[1] C. Reichardt, Chem. Rev. 94 (1994) 2319.
[2] B.P. Johnson, B. Gabrielsen, M. Matulenko, J.G. Dorsey, C. Reichardt, Anal. Lett. 19 (1986) 939.
[3] C. Reichardt, Angew. Chem. Internat. Edit. 4 (1965) 29.
[4] H. Langhals, Angew. Chem. Internat. Edit. 21 (1982) 724.
[5] C. Reichardt, Angew. Chem. Internat. Edit. 18 (1979) 98.
[6] I. Jano, J. Chim. Phys. 89 (1992) 1951.
[7] D.V. Matyushov, R. Schmid, B.M. Ladanyi, J. Phys. Chem. B 101 (1997) 1035.
[8] B.C. Perng, M.D. Newton, F.O. Raineri, H.L. Friedman, J. Chem. Phys. 104 (1996) 7177.
[9] W. Bartkowiak, J. Lipinski, J. Phys. Chem. A 102 (1998) 5236.
[10] J. Lobaugh, P.J. Rossky, J. Phys. Chem. A 103 (1999) 9432.
[11] J. Lobaugh, P.J. Rossky, J. Phys. Chem. A 104 (2000) 899.
[12] S.R. Mente, M. Maroncelli, J. Phys. Chem. B 103 (1999) 7704.
[13] W. Liptay, Z. Naturforsch., Part A 20a (1965) 1441.
[14] A. Schweig, C. Reichardt, Z. Naturforsch., Part A 21a (1966) 1373.
[15] M.T. Carter, R.A. Osteryoung, R.W. Murray, Anal. Chem. 68 (1996) 918.
[16] K.A. Zachariasse, N.V. Phuc, B. Kozankiewicz, J. Phys. Chem. 85 (1981) 2676.
[17] T. Ishida, P.J. Rossky, J. Phys. Chem. A 105 (2001) 558.
[18] J.B. Foresman, A. Frisch, Exploring Chemistry with Electronic Structure Methods, 2nd ed., Gaussian, Pittsburgh, 1995.
[19] J.B. Foresman, M. Head-Gordon, J.A. Pople, M.J. Frisch, J. Phys. Chem. 96 (1992) 135.
[20] M.A. Smith, P.G. Jasien, J. Mol. Struct. (Theochem) 429 (1998) 131.
[21] M.W. Wong, M.J. Frisch, K.B. Wiberg, J. Am. Chem. Soc. 113 (1991) 4776.
[22] L. Onsager, J. Am. Chem. Soc. 58 (1936) 1486.
[23] Gaussian 94, Revision B.1, M.J. Frisch, G.W. Trucks, H.B. Schlegel, P.M.W. Gill, B.G. Johnson, M.A. Robb, J.R. Cheeseman, T. Keith, G.A. Petersson, J.A. Montgomery, K. Raghavachari, M.A. Al-Laham, V.G. Zakrzewski, J.V. Ortiz, J.B. Foresman, J. Cioslowski, B.B. Stefanov, A. Nanayakkara, M. Challacombe, C.Y. Peng, P.Y. Ayala, W. Chen, M.W. Wong, J.L. Andres, E.S. Replogle, R. Gomperts, R.L. Martin, D.J. Fox, D.J. Defrees, J. Baker, J.J.P. Stewart, M. Head-Gordon, C. Gonzalez, J.A. Pople, Gaussian, Inc., Pittsburgh, PA, 1995.
[24] MacSpartan Plus, Wavefunction, Inc., Irvine, CA.
[25] W.J. Hehre, R. Ditchfield, J.A. Pople, J. Chem. Phys. 56 (1972) 2257.
[26] M.J. Frisch, J.A. Pople, J.S. Binkley, J. Chem. Phys. 80 (1984) 3265.
[27] D.R. Lide (Ed.), CRC Handbook of Chemistry and Physics, 74th ed., CRC Press, Boca Raton, 1993, pp. 8–57.
[28] R. Allmann, Z. Kristallogr. 128 (1969) 115.
[29] H. Ågren, S. Knuts, K.V. Mikkelsen, H.J.A. Jensen, Chem. Phys. 159 (1992) 211.
[30] Y. Zong, J.L. McHale, J. Chem. Phys. 107 (1997) 2920.
[31] S.A. Kovalenko, N. Eilers-Konig, T.A. Senyushkina, N.P. Ernsting, J. Phys. Chem. A, 105 (2001) 4834.
[32] L.L. Weber, P.G. Jasien, unpublished results.
[33] S.F. Boys, F. Bernardi, Molec. Phys. 19 (1970) 553.
[34] N.E. Levinger, A.E. Johnson, G.C. Walker, P.F. Barbara, Chem. Phys. Lett. 196 (1992) 159.